



## Plasma-catalytic methane conversion with carbon dioxide in dielectric barrier discharges

Jan Sentek<sup>a</sup>, Krzysztof Krawczyk<sup>a</sup>, Michał Młotek<sup>a,\*</sup>, Małgorzata Kalczewska<sup>a</sup>, Thorsten Kroker<sup>b</sup>, Torsten Kolb<sup>b</sup>, Andreas Schenk<sup>b</sup>, Karl-Heinz Gericke<sup>b</sup>, Krzysztof Schmidt-Szałowski<sup>a</sup>

<sup>a</sup>Warsaw University of Technology, Faculty of Chemistry ul. Noakowskiego 3, 00-664 Warszawa, Poland

<sup>b</sup>Institute of Physical and Theoretical Chemistry Braunschweig 38106, Germany

### ARTICLE INFO

#### Article history:

Received 13 August 2009

Received in revised form 12 October 2009

Accepted 17 October 2009

Available online 29 October 2009

#### Keywords:

Methane conversion

Carbon dioxide

Barrier discharge

Catalyst

### ABSTRACT

The hybrid plasma-catalytic system was tested for the mixture of methane and CO<sub>2</sub> conversion at the pressure of 1.2 bar with the use of a dielectric barrier discharge (DBD) reactor powered at the frequency of 5.7–6 kHz. Three kinds of catalytic packing were examined: alumina ceramic carrier (Al<sub>2</sub>O<sub>3</sub>) and two catalysts, i.e. Ag/Al<sub>2</sub>O<sub>3</sub> and Pd/Al<sub>2</sub>O<sub>3</sub>. The effects of temperature (120–290 °C), [CO<sub>2</sub>]:[CH<sub>4</sub>] molar ratio in the inlet gas mixtures (CH<sub>4</sub> + CO<sub>2</sub> + Ar), gas flow rate, and specific energy on the conversion were studied. Hydrogen, carbon oxide, hydrocarbons (ethane, ethylene + acetylene fraction, propane, propylene, n-butane, and i-butane), and alcohols (methanol and ethanol) were identified in the outlet gas. Among the organic gaseous products, ethane was dominant over the entire parameter range under examination. Non-volatile products (carbon, macromolecular substances) formed a visible deposit on the quartz dielectric barrier and metal electrode surfaces. With the Pd/Al<sub>2</sub>O<sub>3</sub> catalyst, the overall methane conversion was 30–50% and the methane conversion to C<sub>2</sub>–C<sub>4</sub> hydrocarbons reached 22%.

© 2009 Elsevier B.V. All rights reserved.

## 1. Introduction

Non-thermal (non-equilibrium) plasma conversion of methane and other light hydrocarbons is regarded as a new way for a profitable production of valuable chemicals, such as unsaturated hydrocarbons, aromatics, oxygenates. Especially, the hybrid plasma-catalytic systems for oxidative and non-oxidative methane processing have attracted a growing interest. Among a variety of plasma techniques, corona and dielectric barrier discharges (DBD) proved their usefulness in these experiments. When using these kinds of discharges, it is easy to fill the entire discharge space with a bed of catalyst particles of desired size, shape and composition. Owing to the proper reaction volume configuration, the time span between active species generation by plasma and their contact with active centers of a solid catalyst may be minimized. The ozone synthesis in DBD was one of the first processes, in which different kinds of packing of dielectric or metal particles placed inside the discharge zone were tested. It was shown that some dielectric materials, e.g. silica, may strongly affect the mechanism of the ozone synthesis probably due to the surface discharge formation over these particles (e.g. Ref. [1]). These experiments showed that

the interaction of the plasma generated active species (free radicals, excited molecules, ions) with solid surfaces may effectively influence the reaction pathways.

## 2. Background

Over the last decade, the conversion of methane with carbon dioxide, both unwanted “greenhouse” gases, became the object of wide studies aimed at the direct synthesis of higher hydrocarbons, liquid fuels, methanol, formaldehyde, and other important oxygenates. Several concepts have been tested for improving the efficiency of methane and carbon dioxide utilization. The formation of C<sub>2</sub> (and higher) hydrocarbons and oxygenates by catalytic coupling of methane with CO<sub>2</sub> requires high temperatures and specific catalysts, because of the high energy of C–H bonds and easy carbon (coke) formation on the catalyst surface. Nowadays, these methods cannot compete with the commercial processes of the catalytic methane conversion via synthesis gas, even though the latter are expensive because of high energy consumption. Hybrid systems, where the action of non-equilibrium plasma is combined with a catalyst accelerating the selected reactions between the active gas species at low temperatures, may be a perspective way for overcoming these obstacles. The role of catalysts in such hybrid systems is specific [2,3]. Short living active species produced by plasma (excited molecules, radicals, ions) are

\* Corresponding author.

E-mail address: [michalm74pw@gmail.com](mailto:michalm74pw@gmail.com) (M. Młotek).

involved in the reactions induced by the catalyst. Owing to the high rate of this kind of reactions, they proceed mostly on the active centres placed at the external surface of catalyst particles.

In recent years, the hybrid plasma-catalytic systems based on DBD were the object of numerous studies. The catalytic effect of metal electrodes on the methane conversion to hydrogen in DBD was observed by Spiess et al. [4]. The conversion of methane in a pure methane stream and in mixtures with non-oxidative gases (noble gases, hydrogen) was examined in DBD with the use of various catalysts, e.g. zeolites [5], Pt/ $\gamma$ - $\text{Al}_2\text{O}_3$  [6], Ru/ $\gamma$ - $\text{Al}_2\text{O}_3$  [7], Ru/ $\text{TiO}_2$  [8], and Cu/ $\text{ZnO}/\text{Al}_2\text{O}_3$  [9]. Ni/ $\gamma$ - $\text{Al}_2\text{O}_3$  [10–13] and Cu/ $\text{ZnO}/\text{Al}_2\text{O}_3$  [14,15] catalysts were tested for the partial oxidation and steam conversion of methane by DBD. Numerous studies were aimed at producing unsaturated hydrocarbons, alcohols and other oxygenates from methane and carbon dioxide. For these experiments, DBDs were combined with zeolites [16,17], Ni/ $\gamma$ - $\text{Al}_2\text{O}_3$  [18], Cu/ $\text{ZnO}/\text{Al}_2\text{O}_3$  [9] etc. Corona discharges were also examined in hybrid plasma-catalytic systems, e.g. for non-oxidative methane coupling on zeolite catalysts [19]. This kind of discharges was also used for oxidative methane coupling to ethylene on Pd/Y-zeolite and Ag/Pd/Y-zeolite [20]. Conversion of methane with carbon dioxide to  $\text{C}_2$  hydrocarbons was studied in pulsed corona discharges combined with selected catalysts based on  $\text{La}_2\text{O}_3/\gamma$ - $\text{Al}_2\text{O}_3$  [21]. A review of researches on the methane conversion with  $\text{CO}_2$  in hybrid plasma-catalytic systems was given by Istadi [22]. Silver and palladium catalysts supported on alumina ceramics were the objects of the present study on the  $\text{CH}_4 + \text{CO}_2$  conversion by the hybrid plasma-catalytic system with the use of DBD.

### 3. Experimental section

Three kinds of packing were selected for this experiment: (1) commercial alumina ceramic carrier for the high temperature Ni catalyst (referred to as  $\text{Al}_2\text{O}_3$ ), (2), silver catalyst ( $\text{Ag}/\text{Al}_2\text{O}_3$ ), and palladium catalyst ( $\text{Pd}/\text{Al}_2\text{O}_3$ ). The supported catalysts (each containing about 3 wt.% of metal) were obtained by impregnation of the alumina-ceramic particles (1.0–2.0 mm in size) with aqueous solutions of silver nitrate or palladium nitrate, dried and calcined in ambient air at  $400^\circ\text{C}$  for 4 h and reduced with hydrogen at  $400^\circ\text{C}$  for 12 h. The portion of 80 ml of the catalyst was packed into the reactor volume. The BET adsorption isotherm was used for carrier and catalysts surface determination. Measurements were performed using Micromeritics 2020 apparatus by absorption of  $\text{N}_2$  at liquid nitrogen temperature, with the  $P/P_0$  ratio in the range 0.05–0.3 (Table 1). The main components of the calcined catalysts were determined by XRD studies with the use of  $\text{Seifert GmbH}$  type Bragg-Brentano HZG – 4 ( $\text{CuK}\alpha$ ,  $\lambda = 1.54 \text{ \AA}$ ). The results are presented in Fig. 1. Traces of Ni compounds were present in this material. No changes were noticed when the catalysts after usage in the DBD reactor were examined.

A quartz-glass reactor with an internal diameter of 26 mm was used with the inner high-voltage electrode made of aluminum (Fig. 2). The discharge gap between this electrode and the quartz tube, used as the dielectric barrier, was about 3 mm wide. The grounded electrode was made from silver-paste deposited on the outer surface of the quartz tube. The reactor was powered by the frequency of 5.7–6 kHz and was operated at the pressure of 1.2 bar. The temperature was controlled by the outer electrical heater and

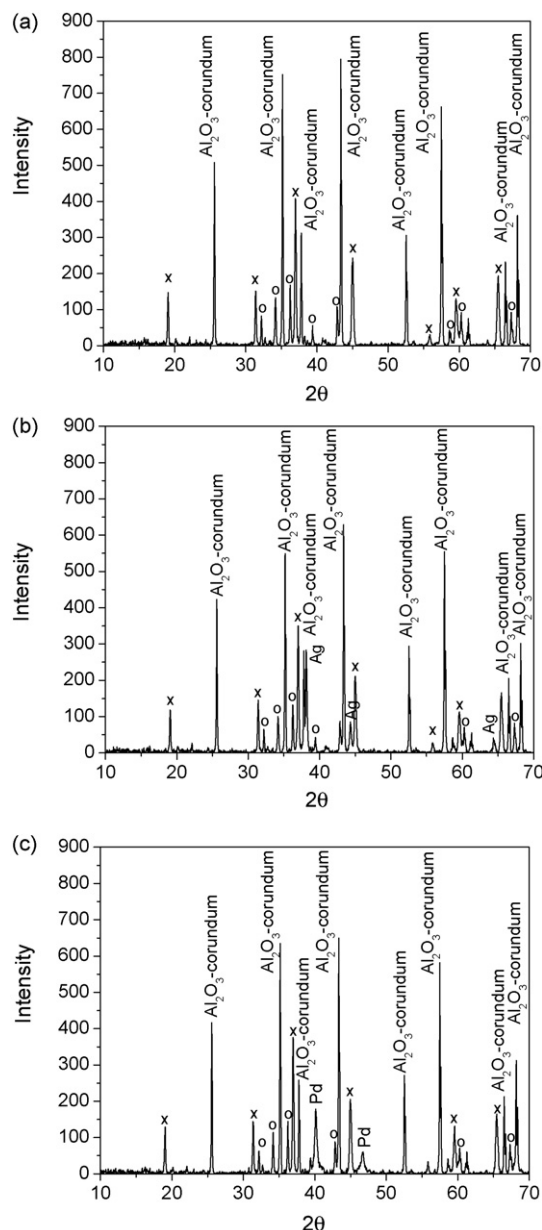


Fig. 1. XRD study of reactor packing after calcinations. (a) Alumina ceramic; (b)  $\text{Ag}/\text{Al}_2\text{O}_3$  (c)  $\text{Pd}/\text{Al}_2\text{O}_3$ ; x –  $\text{NiAl}_2\text{O}_4$  (Nickel aluminum oxide); o –  $\text{CaAl}_{12}\text{O}_{19}$  (Hibonite).

was measured with a thermocouple at the surface of the reactor wall. Methane 99.5%, carbon dioxide 99.99%, and argon 99.999% were the components of the feeding gas mixtures. The gas flow rates were controlled by mass controllers. The components of inlet and outlet gases were determined by chromatographic method (GC Agilent 6890N instrument). The concentration of a given component in the inlet stream or that of one after the reactor did not differ from the average by more than  $\pm 5\%$ . The share of other products, i.e. higher than  $\text{C}_4$  and that of non-volatile products, mainly soot, were computed from the carbon balance.

#### 3.1. Parameters and definitions

$W_0[\text{CH}_4]$ ,  $W_0[\text{CO}_2]$ ; (mmol/h) – methane and carbon dioxide flow rates at the inlet

$W[\text{CH}_4]$ ,  $W[\text{CO}_2]$ ,  $W[\text{H}_2]$ ,  $W[\text{C}_m\text{H}_n]$ ; (mmol/h) – methane, carbon, dioxide, hydrogen and  $\text{C}_m\text{H}_n$  hydrocarbons flow rates, respectively, at the outlet

Table 1

Specific surfaces ( $S_{\text{BET}}$ ) of packings from BET measurement.

Packing	$S_{\text{BET}}$ ( $\text{m}^2/\text{g}$ )
$\text{Al}_2\text{O}_3$	2.3
$\text{Ag}/\text{Al}_2\text{O}_3$	2.1
$\text{Pd}/\text{Al}_2\text{O}_3$	2.5

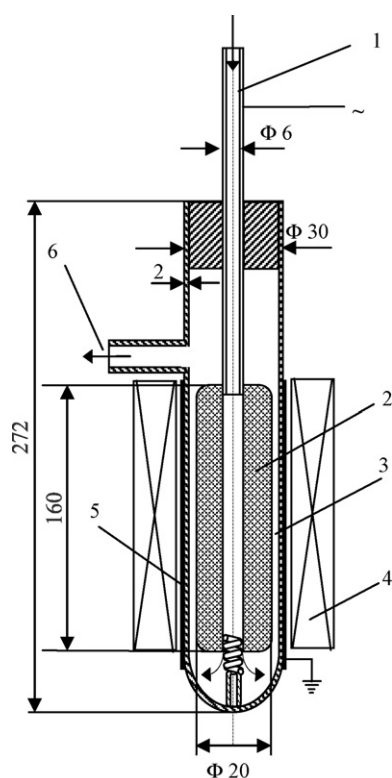


**Fig. 2.** Plasma reactor: 1 – gas inlet, 2 – high-voltage electrode, 3 – discharge gap (3 mm), 4 – electric heater, 5 – grounded electrode, 6 – gas outlet.

N – unidentified volatile (higher than C<sub>4</sub>) and non-volatile products

W<sub>C</sub> (mmol/h) – Carbon fixed in N (from C balance)

P (W) – power computed from oscilloscope measurements of current and voltage in the reactor circuit,

- Overall methane conversion:  $X[\text{CH}_4] = \frac{W_0[\text{CH}_4] - W[\text{CH}_4]}{W_0[\text{CH}_4]}$
- Overall carbon dioxide conversion:  $X[\text{CO}_2] = \frac{W_0[\text{CO}_2] - W[\text{CO}_2]}{W_0[\text{CO}_2]}$
- Methane conversion to C<sub>m</sub>H<sub>n</sub>:  $X[\text{CH}_4 \rightarrow \text{C}_m\text{H}_n] = \frac{nW[\text{C}_m\text{H}_n]}{W_0[\text{CH}_4]}$

**Table 2**

Conversion of methane and carbon dioxide to individual products [%]. T = 240 °C, P = 18–19 W.

	Without packing	Al <sub>2</sub> O <sub>3</sub>	Pd/Al <sub>2</sub> O <sub>3</sub>	Ag/Al <sub>2</sub> O <sub>3</sub>	Without packing	Al <sub>2</sub> O <sub>3</sub>	Pd/Al <sub>2</sub> O <sub>3</sub>	Ag/Al <sub>2</sub> O <sub>3</sub>	Without packing	Al <sub>2</sub> O <sub>3</sub>	Pd/Al <sub>2</sub> O <sub>3</sub>	Ag/Al <sub>2</sub> O <sub>3</sub>
CO <sub>2</sub> : CH <sub>4</sub>			<b>1</b>				<b>1</b>				<b>2</b>	
V, NL/h			<b>2</b>				<b>1</b>				<b>1</b>	
X[CH <sub>4</sub> ]	34.3	36.5	32.0	33.6	56.8	52.2	45.2	49.0	58.0	54.7	50.9	52.0
X[CO <sub>2</sub> ]	18.4	21.9	20.5	20.5	35.7	31.0	28.3	29.6	33.0	26.0	28.1	29.0
X[CH <sub>4</sub> → H <sub>2</sub> ]	13.9	13.8	14.4	13.5	26.7	23.7	20.7	21.5	32.8	28.2	29.0	28.7
X[CH <sub>4</sub> → CO]	5.91	6.84	13.7	9.68	21.2	18.7	23.3	19.3	39.6	38.1	40.0	37.9
X[CH <sub>4</sub> → C <sub>2</sub> H <sub>6</sub> ]	7.58	8.76	13.2	8.76	10.0	10.2	15.0	9.75	7.40	8.10	9.45	7.58
X[CH <sub>4</sub> → C <sub>2</sub> H <sub>2,4</sub> ]	1.10	0.47	0.06	0.48	0.48	0.55	0.09	0.57	0.20	0.38	0.00	0.28
X[C <sub>2</sub> ]	8.67	9.24	13.28	9.24	10.5	10.8	15.1	10.3	7.60	8.48	9.45	7.86
X[CH <sub>4</sub> → C <sub>3</sub> H <sub>8</sub> ]	3.77	4.18	3.53	3.97	5.47	5.49	4.49	5.03	3.56	4.00	2.70	3.34
X[CH <sub>4</sub> → C <sub>3</sub> H <sub>6</sub> ]	0.19	0.19	0.09	0.20	0.27	0.27	0.13	0.26	0.10	0.19	0.00	0.10
X[C <sub>3</sub> ]	3.96	4.37	3.62	4.17	5.74	5.77	4.62	5.29	3.66	4.19	2.70	3.43
X[CH <sub>4</sub> → n-C <sub>4</sub> H <sub>10</sub> ]	1.39	1.55	1.13	1.48	2.14	2.26	1.50	2.05	1.14	1.53	0.78	1.12
X[CH <sub>4</sub> → i-C <sub>4</sub> H <sub>10</sub> ]	1.39	1.35	0.80	1.22	2.74	2.11	1.08	1.82	1.41	1.41	0.52	1.04
X[C <sub>4</sub> ]	2.77	2.90	1.93	2.71	4.88	4.36	2.57	3.86	2.55	2.94	1.30	2.16
X[CH <sub>4</sub> → MeOH]	0.64	1.62	0.78	1.57	0.97	1.18	0.94	1.22	1.27	1.63	1.10	1.62
X[CH <sub>4</sub> → EtOH]	0.20	0.19	0.10	0.17	0.23	0.27	0.13	0.25	0.20	0.30	0.13	0.26
X <sub>C</sub>	12.1	11.3	0	6.10	13.3	11.2	0	8.75	3.18	0	0	0

V – flow rate at the inlet.

4. Methane conversion to higher than C<sub>4</sub> and non-volatile products:  $X_C = \frac{W_C}{W_0[\text{CH}_4]}$

5. Methane conversion to CO:  $X[\text{CH}_4 \rightarrow \text{CO}] = \frac{W[\text{CO}_2] + W[\text{CO}] - W_0[\text{CO}_2]}{W_0[\text{CH}_4]}$

6. Methane conversion to H<sub>2</sub>:  $X[\text{CH}_4 \rightarrow \text{H}_2] = \frac{W[\text{H}_2]}{2W_0[\text{CH}_4]}$

7. Shares of hydrogen fixed in individual components of the outlet gas:  $H_x = \frac{nW[\text{C}_m\text{H}_n]}{4W_0[\text{CH}_4]}$

8. Shares of hydrogen fixed in individual reaction products:  $H_y = \frac{nW[\text{C}_m\text{H}_n]}{4W_0[\text{CH}_4] - 4W[\text{CH}_4]}$

9. Specific energy; [J/mmolCH<sub>4</sub>]:  $SE = \frac{P \times 3600}{W_0[\text{CH}_4]}$

## 4. Results

Three kinds of packing were tested in this experiment: alumina ceramic (commercial) carrier (Al<sub>2</sub>O<sub>3</sub>) and two catalysts Ag/Al<sub>2</sub>O<sub>3</sub> and Pd/Al<sub>2</sub>O<sub>3</sub>. The effects of temperature (over 120–290 °C), [CO<sub>2</sub>]:[CH<sub>4</sub>] molar ratio in the inlet gas mixtures (CH<sub>4</sub> + CO<sub>2</sub> + Ar), gas flow rate, and specific energy on the conversion efficiency were examined. The gaseous products determined by chromatographic analysis are specified in Table 2. These were: hydrogen, carbon oxide, hydrocarbons (ethane, fraction composed of ethylene + acetylene, propane, propylene, n-butane, and i-butane), and alcohols (methanol and ethanol). Among the organic products, ethane was dominant over the entire parameter ranges under examination. During the reaction run, non-volatile products (coke, macromolecular substances) formed a thin but visible film of deposit on the quartz dielectric barrier and metal electrode surfaces. The generation rate of these deposits was strongly affected by the inlet gas composition. It was much higher when the [CO<sub>2</sub>]:[CH<sub>4</sub>] ratio was 1, than when it was 2. Thus, the higher concentration of CO<sub>2</sub>, that is the oxidizing component in the gas mixture, reduced the solid product formation. A similar effect of oxidants (CO<sub>2</sub>, H<sub>2</sub>O, O<sub>2</sub>), which prevent the catalyst coking is known from the high temperature catalytic methane conversion with carbon dioxide, water vapor etc. The presence of solid particles in DBD may reduce the formation of non-volatile products [23]. In our earlier experiments with the hybrid gliding discharge system, the Pt and Pd catalysts prevented the carbon deposit formation [3]. The main results of the present study may be shortly characterized as follows:

#### 4.1. The effects of reactor packing (Table 2)

- Comparing the products generated with the  $\text{Al}_2\text{O}_3$  packing to those without packing, only few changes could be noticed. The amounts of C2 hydrocarbons (mainly ethane), C3 hydrocarbons and methanol were slightly increased and that of C4 hydrocarbons decreased. The  $>\text{C}_4$  hydrocarbons and deposit formation was slightly reduced.
- In the presence of the  $\text{Ag}/\text{Al}_2\text{O}_3$  catalyst, the overall conversion of  $\text{CH}_4$  and  $\text{CO}_2$  was similar (except few cases) to that without packing. With this catalyst, slightly higher conversion to C2 hydrocarbons and alcohols (methanol) were noticed in contrast with a slightly lower conversion to C4 hydrocarbons. The  $>\text{C}_4$  hydrocarbons and deposit formation was markedly reduced.
- With the use of the  $\text{Pd}/\text{Al}_2\text{O}_3$  catalyst, the overall methane conversion was found slightly lower than without packing. Nevertheless, the changes in the product composition were significant. The amount of C2 hydrocarbons (mainly ethane) was increased in contrast with these of C3 and C4 hydrocarbons, which were reduced. These changes were stronger over the higher temperature range (240–290 °C). The  $>\text{C}_4$  hydrocarbons and deposit formation radically slowed down.

The effects of each kind of packing are shown in Figs. 3–6, and the maximum conversion values noticed for the individual products during the entire experiment, are collected in Table 3. For discussing the experiment with  $\text{Pd}/\text{Al}_2\text{O}_3$  catalyst, the hydrogen balance was computed. In the case of the mixture of molar ratio  $[\text{CO}_2]:[\text{CH}_4] = 1$  and the overall flow rate of 1 NL/h ( $0.25\text{CH}_4 + 0.25\text{CO}_2 + 0.5\text{Ar}$ ), the following hydrogen balance was found. The unconverted fraction of methane contained 45% of hydrogen and the shares of hydrogen fixed in the individual

products were: 20% in  $\text{H}_2$ , 11% in C2 hydrocarbons, 3% in C3 hydrocarbons, approx. 1.5% in C4 hydrocarbons, and approx. 1% in alcohols. The hydrogen balance computed on the basis of other experiments with  $[\text{CO}_2]:[\text{CH}_4] = 1$  is shown in Fig. 3, where shares (Hx) of hydrogen fixed in individual components of the outlet gas are depicted. Additionally, in Fig. 4, shares (Hy) of hydrogen fixed in individual reaction products are shown (here the share of unconverted methane is omitted).

#### 4.2. The effect of temperature (over the range of 120–290 °C; Fig. 5)

- The temperature did not affect the overall methane conversion, however a shift in individual product generation could be noticed. This effect was the most distinct when Pd catalyst was used. In the presence of this catalyst, the increased methane conversion to ethane (up to 15%) was observed over the higher temperature range (240–290 °C).
- In contrast with the increased conversion to C2 hydrocarbons, the conversion to CO and alcohols was strongly reduced at higher temperatures with Pd catalyst.
- Except the experiment with the Pd catalyst, an increased generation of C4 hydrocarbons and a diminished one of alcohols were observed in the higher temperature range (up to 290 °C).

#### 4.3. The effect of inlet gas composition ( $\text{CH}_4 + \text{CO}_2 + \text{Ar}$ ; Table 2)

- The shift in the  $[\text{CO}_2]:[\text{CH}_4]$  ratio from 1 to 2 caused only weak changes of the overall conversion of  $\text{CH}_4$  and  $\text{CO}_2$ .
- When the Pd catalyst was used, the methane conversion to hydrogen increased (e.g. from 21% to 29%) due to the increased  $[\text{CO}_2]:[\text{CH}_4]$  ratio from 1 to 2. (However, the maximum conversion to hydrogen was observed at 33% without packing.)

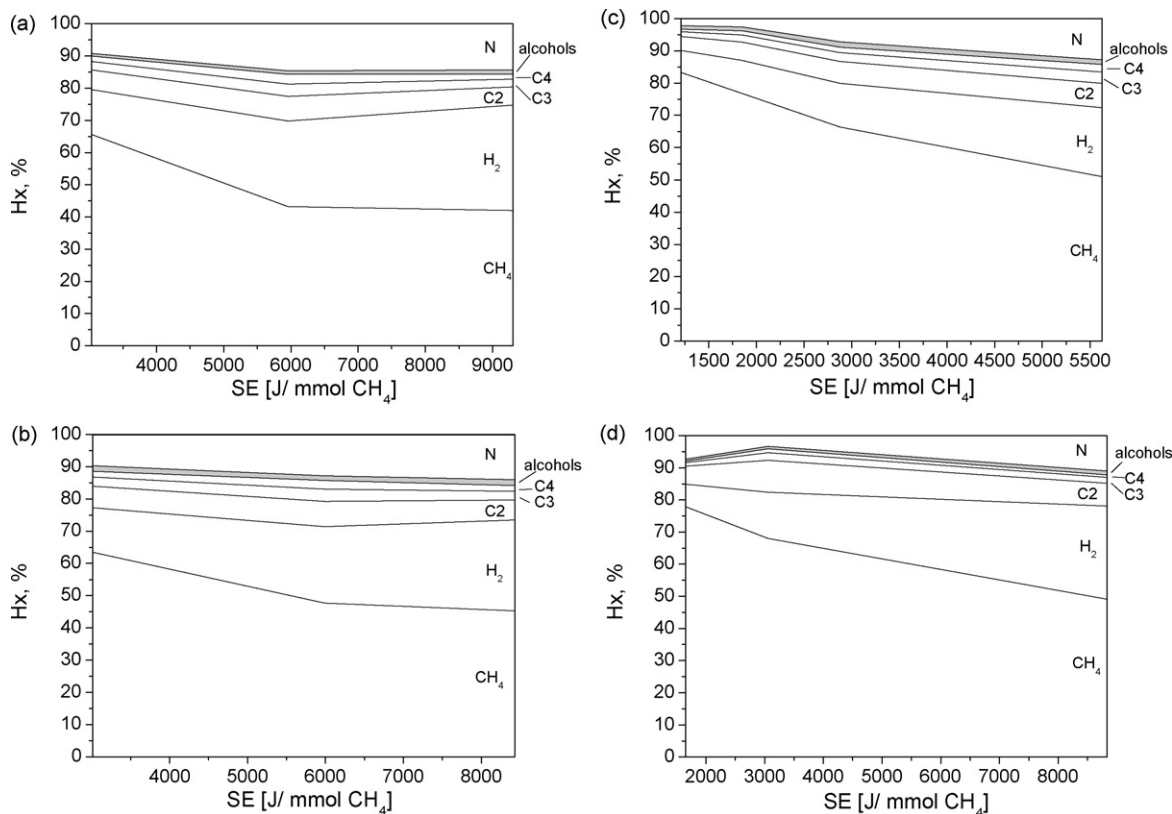
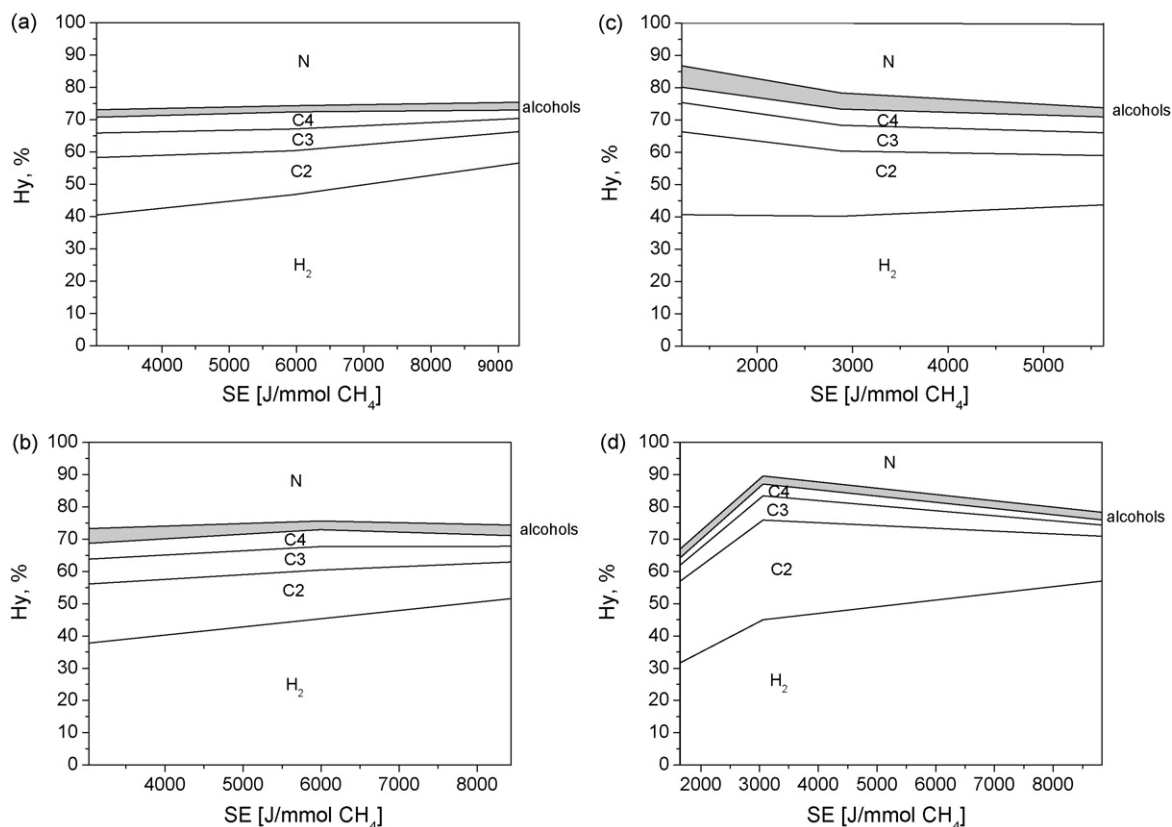


Fig. 3. Shares of hydrogen (Hx) fixed in components of the outlet stream for different specific energies SE. Experiment conditions:  $[\text{CO}_2]:[\text{CH}_4] = 1$ , Temp. 240 °C. (a) Without packing, (b) alumina ceramic, (c)  $\text{Ag}/\text{Al}_2\text{O}_3$ , (d)  $\text{Pd}/\text{Al}_2\text{O}_3$ .



**Fig. 4.** Shares of hydrogen (Hy) fixed in individual reaction products (methane is omitted) for different specific energies SE. Experiment conditions:  $[\text{CO}_2]:[\text{CH}_4] = 1$ , Temp.  $240^\circ\text{C}$ . (a) Without packing, (b) alumina ceramic, (c)  $\text{Ag}/\text{Al}_2\text{O}_3$ , (d)  $\text{Pd}/\text{Al}_2\text{O}_3$ .

- With the Pd catalyst, the methane conversion to CO also increased (e.g. from 23% to 40%) when the mixture of  $[\text{CO}_2]:[\text{CH}_4] = 2$  was used.
- The methane conversion to C2, C3, and C4 hydrocarbons was significantly reduced in the mixture with  $[\text{CO}_2]:[\text{CH}_4] = 2$ . This effect was observed in all experiments, with and without packing.
- When the  $\text{Al}_2\text{O}_3$  or Ag catalyst was used, the conversion to methanol increased up to 1.6% owing to the higher  $[\text{CO}_2]:[\text{CH}_4]$  ratio.

#### 4.4. The effect of gas flow rate ( $V = 1$ or $2\text{N L/h}$ ; Table 2)

- The conversion of both reagents  $\text{CH}_4$  and  $\text{CO}_2$  to the main products was reduced when the gas flow rate was increased from 1 to  $2\text{N L/h}$  (at  $[\text{CO}_2]:[\text{CH}_4] = 1$ ).
- With the empty reactor (without packing), the ethylene + acetylene fraction was more abundant at the higher flow rate.
- In the presence of  $\text{Al}_2\text{O}_3$  and the Ag catalyst, the conversion to methanol was increased at the higher flow rate.

#### 4.5. The effect of specific energy per mol $\text{CH}_4$ introduced (SE)

Fig. 6 shows the case of  $[\text{CO}_2]:[\text{CH}_4] = 1$ , the gas flow rate of 1 and  $2\text{N L/h}$ , and the temperature  $240^\circ\text{C}$ .

- $\text{CH}_4$  and  $\text{CO}_2$  conversions were accelerated by increasing SE.
- Amounts of  $\text{H}_2$  and CO in the outlet gas increased parallel to SE in all experiments with and without packing.
- The content of C2, C3, and C4 hydrocarbons in the outlet stream reached a maximum at the medium range of SE.
- The generation of methanol and ethanol only slightly depended on SE, showing a tendency to increase parallel to SE.

## 5. Discussion

For discussing the results of plasma-catalytic reactions, the following simplified scheme of the overall process composed of three stages may be useful.

The first consists of the reagent activation by electron impact or by reactions with atomic and molecular active species:  $\text{H}$ ,  $\text{O}$ ,  $\text{O}^-$ ,  $\text{OH}$ ,  $\text{OH}^-$  [16]. In this way, the first generation of  $\text{C}_1\text{H}_n$  radicals is produced by methane molecule transformations. The following reactions may induce the methane processing (e.g. Ref. [24]):



and in the presence of  $\text{CO}_2$  O radicals are formed:



Moreover, energized electrons may generate a number of other short living active species, e.g. excited molecules at higher electron or vibrational states.

During the second stage, fast homogeneous reactions proceed in the gas phase between the short living active species that have been produced due to reactions of the previous stage.

Reactions induced by the solid surfaces may be treated as the third stage of the overall process. They take place on electrode surfaces and inside the discharge volume, if a packing is used. In the presence of catalyst particles, a chain of molecular processes may proceed including the molecule adsorption on the surface, reactions between the adsorbed species, and desorption of reaction products.

A peculiar character of these processes is the cause of the often made observation that the reaction course depends not only on the

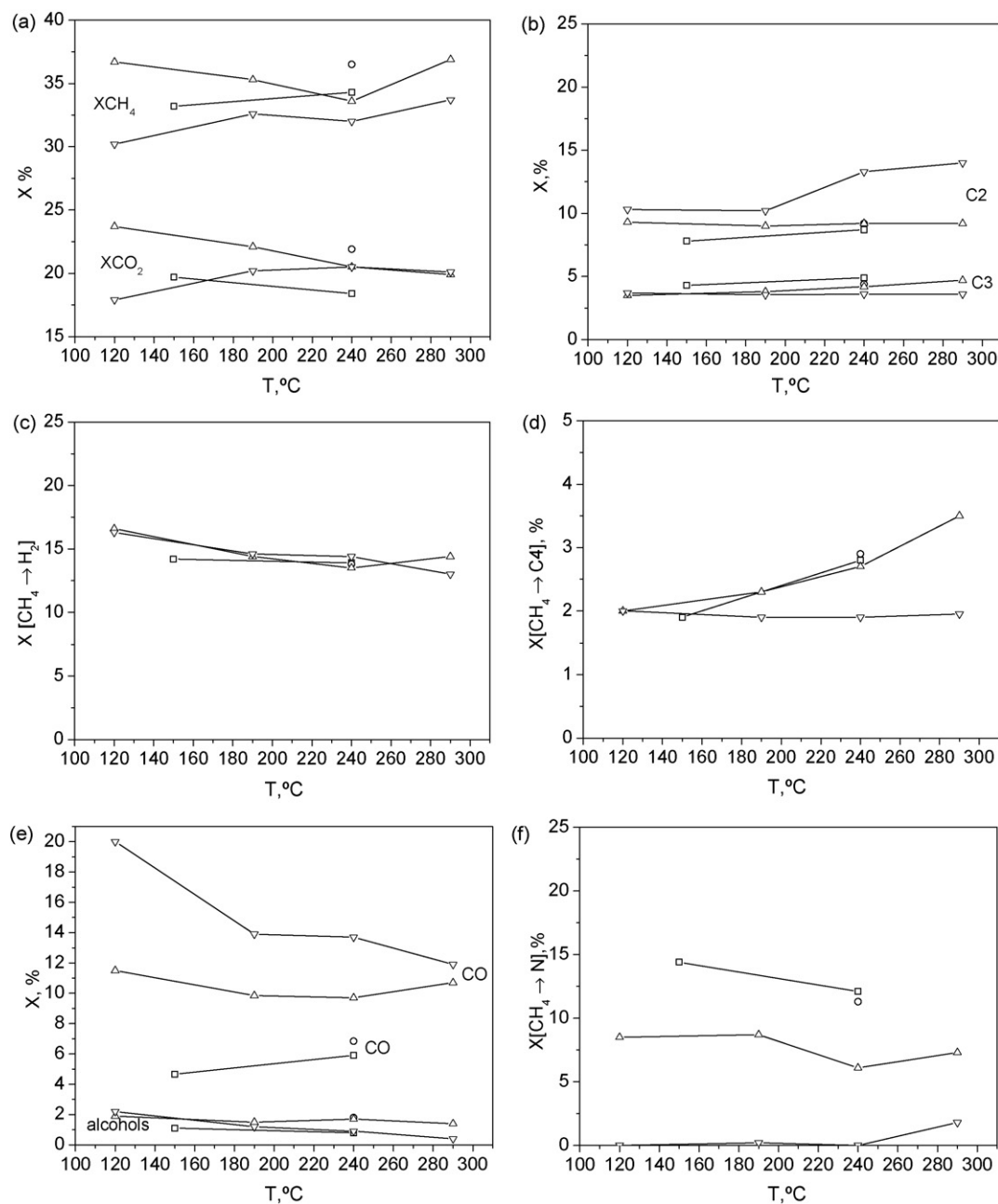


**Fig. 5.** Effect of temperature on the conversion to individual products. Experiment conditions: flow rate 2N L/h, [CO<sub>2</sub>]:[CH<sub>4</sub>] = 1 (0.5CH<sub>4</sub> + 0.5CO<sub>2</sub> + 1Ar), P = 18–19 W. (a) XCH<sub>4</sub> and XCO<sub>2</sub>; (b) X[CH<sub>4</sub> → H<sub>2</sub>]; (c) X[CH<sub>4</sub> → CO] and X[CH<sub>4</sub> → alcohols] (d) X[CH<sub>4</sub> → C<sub>2</sub>] and X[CH<sub>4</sub> → C<sub>3</sub>]; (e) X[CH<sub>4</sub> → C<sub>4</sub>]; (f) X[CH<sub>4</sub> → N<sub>2</sub>]; □ - without packing, ○ - alumina ceramic, Δ - Ag/Al<sub>2</sub>O<sub>3</sub>, ▽ - Pd/Al<sub>2</sub>O<sub>3</sub>.

discharge conditions and the catalyst's activity but also on the configuration of the reaction volume. The role of catalysts in hybrid systems is specific, because conducting the reactions between short living active species is their main function. When the time elapsing between the active species generation in plasma and their contact with the catalyst's surface is relatively long, most of the fast reactions are terminated in the gas phase. In this case, the catalyst could have no influence on the reactant's transformation (e.g. Ref. [9]).

The structure of DBD reactors is beneficial for developing the plasma-catalytic processes because the catalyst particles are placed inside the discharge zone. Thus, the transfer of the active species generated by plasma to the catalyst surface may be effective. In this case, fast reactions take place on external surfaces of the catalyst particles. Because of the slow diffusion of molecules through porous materials, the internal structure of the catalyst is

of minor importance. There are, however, some obstacles against making use of catalysts in this system. First, it should be taken into account that the presence of solid particles in the discharge zone may disturb the process conditions in different ways, e.g. changing the discharge structure and its character by shifting the current flow from the gas volume to the surface. Thus, the electrical parameters (field strength, current density) in the discharge zone may be significantly changed. Moreover, other process conditions may also be disturbed by the packing, e.g. the hydrodynamics of gas stream and the temperature field. On the other hand, the specific structure of active centres on the catalyst surface may easily be destroyed by the action of energized gas species. Thus, an efficient catalyst should be resistant against this kind of surface reconstruction, which can reduce its activity. Our experiment has shown that the Pd/Al<sub>2</sub>O<sub>3</sub> catalyst may cope with this obstacles.

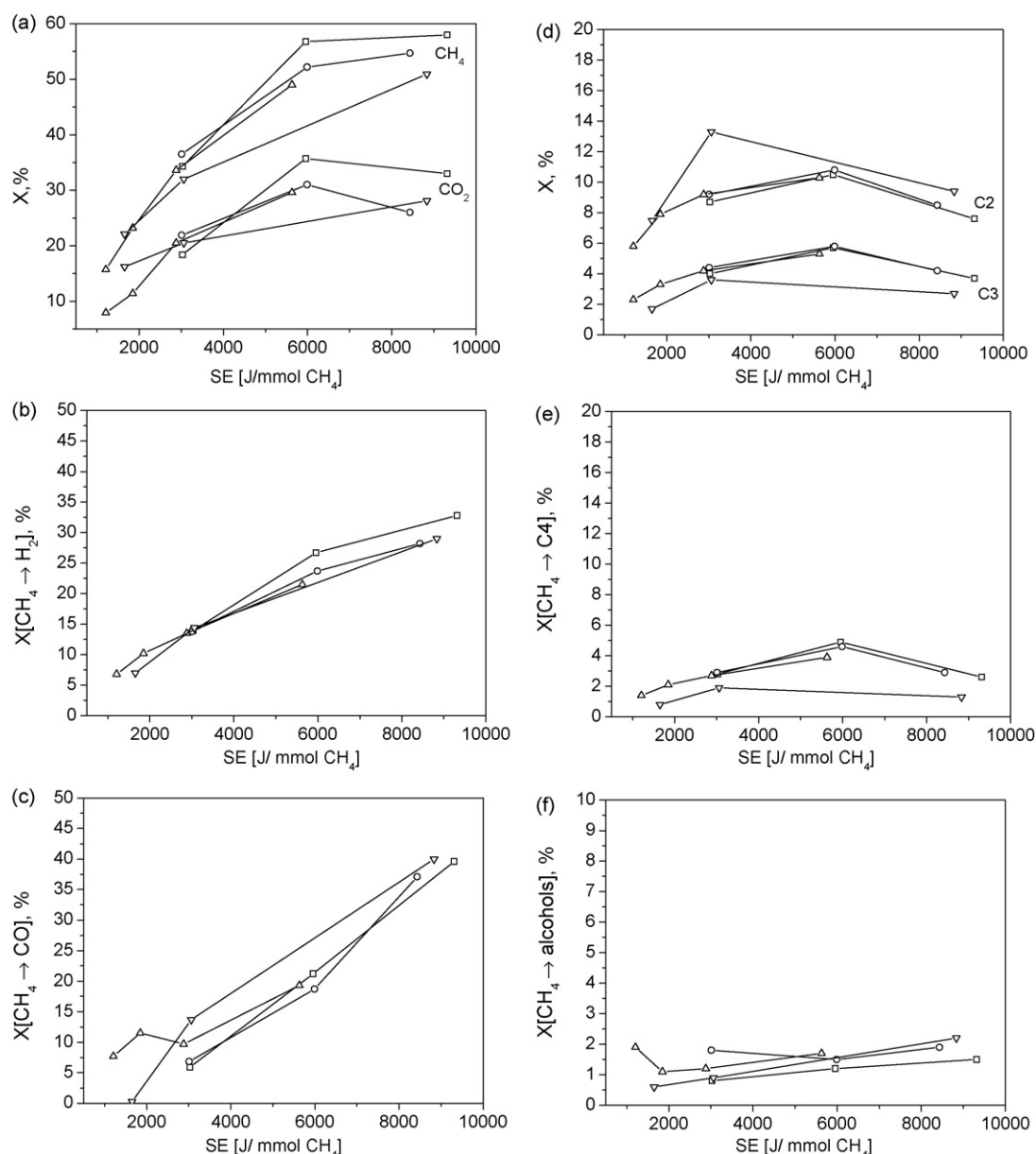


**Fig. 6.** Effect of specific energy SE on the conversion to individual products. Experiment conditions: flow rate 2N L/h.;  $[\text{CO}_2]:[\text{CH}_4] = 1$  ( $0.5\text{CH}_4 + 0.5\text{CO}_2 + 1\text{Ar}$ ), Temp. 240 °C. (a)  $X[\text{CH}_4]$  and  $X[\text{CO}_2]$ ; (b)  $X[\text{CH}_4 \rightarrow \text{H}_2]$ ; (c)  $X[\text{CH}_4 \rightarrow \text{CO}]$ ; (d)  $X[\text{CH}_4 \rightarrow \text{C}_2]$  and  $X[\text{CH}_4 \rightarrow \text{C}_3]$ ; (e)  $X[\text{CH}_4 \rightarrow \text{C}_4]$ ; (f)  $X[\text{CH}_4 \rightarrow \text{alcohols}]$ .  $\square$  – without packing,  $\circ$  – alumina ceramic,  $\Delta$  –  $\text{Ag}/\text{Al}_2\text{O}_3$ ,  $\nabla$  –  $\text{Pd}/\text{Al}_2\text{O}_3$ .

For comparing the results presented here with those of other studies it should be kept in mind that ethane was the most abundant among organic products in all of our experiments with and without packing. The results of other investigations on the methane

conversion with  $\text{CO}_2$  in DBD seem to be similar, e.g. Ref. [25]. Furthermore, on the basis of modeling studies [26] of pure methane conversion by DBD, it was found that at low energy density and low concentrations of electrons bearing energy higher than 6 eV, ethane and propane are the most abundant products. However, when energy density increases, the rate of ethane generation is reduced and acetylene becomes the main product.

In hybrid systems, catalysts can strongly affect the products of the methane conversion by DBD and corona discharges. For example, when NaX zeolite was introduced to the DBD reactor [2], an increased concentration of ethane and propane was observed. At the same time, the soot and polymer deposit formation was significantly reduced. An interesting effect of catalysts was observed in the study on the oxidative methane conversion (with  $\text{H}_2$  and  $\text{O}_2$ ) in DC corona. The product composition was radically shifted from acetylene to ethylene and ethane, when a Pd/Y-zeolite catalyst was used [20]. A similar effect was observed for non-oxidative methane coupling in gliding discharges, where owing to

**Table 3**

Maximum conversion values found in all experiment series with different catalysts and different  $[\text{CO}_2]:[\text{CH}_4]$  ratio.

Conversion	%	Packing	$[\text{CO}_2]:[\text{CH}_4]$
$X[\text{CH}_4]$	58	None	2:1
$X[\text{CO}_2]$	36	None	1:1
$X[\text{CH}_4 \rightarrow \text{H}_2]$	33	None	2:1
$X[\text{CH}_4 \rightarrow \text{CO}]$	40	Pd or None	2:1
$X[\text{CH}_4 \rightarrow \text{C}_2\text{--C}_4]$	22	Pd	1:1
$X[\text{CH}_4 \rightarrow \text{C}_2]$	15	Pd	1:1
$X[\text{CH}_4 \rightarrow \text{C}_3]$	5.8	$\text{Al}_2\text{O}_3$ or None	1:1
$X[\text{CH}_4 \rightarrow \text{C}_4]$	4.9	None	1:1
$X[\text{CH}_4 \rightarrow \text{alcohols}]$	1.9	$\text{Al}_2\text{O}_3$ or Ag	2:1

the presence of Pd catalyst, ethylene was generated instead of acetylene, which was the main product of the single plasma process, i.e. without catalyst [3]. Thus, the result of our present investigation is consistent with those observed in the aforementioned studies. Our experiments have shown that owing to the Pd/Al<sub>2</sub>O<sub>3</sub> catalyst, the amount of evolved C<sub>2</sub> hydrocarbons (mainly ethane) may be increased, whereas that of C<sub>3</sub> and C<sub>4</sub> hydrocarbons diminished. It is also worth mentioning that in the presence of this catalyst, non-volatile deposit formation was radically reduced [27].

## 6. Conclusion

1. The conversion of methane with CO<sub>2</sub> was effectively conducted in a hybrid plasma-catalytic system with the use of a DBD reactor operated at the pressure of 1.2 bar over the temperature range of 120–290 °C. The action of discharges was studied in the presence of an alumina ceramic carrier (Al<sub>2</sub>O<sub>3</sub>) and two catalysts, namely Ag/Al<sub>2</sub>O<sub>3</sub> and Pd/Al<sub>2</sub>O<sub>3</sub>.
2. Hydrogen, carbon oxide, hydrocarbons (ethane, fraction composed of ethylene + acetylene, propane, propylene, n-butane, and i-butane), and alcohols (methanol and ethanol) were found in the outlet stream over the entire range of process conditions. Ethane was the main component among the organic products. Non-volatile products (coke, macromolecular substances) formed a deposit inside the reactor.
3. A Pd/Al<sub>2</sub>O<sub>3</sub> catalyst was the most effective among the tested kinds of packing. With this catalyst, the overall methane conversion was slightly lower than without packing, however, the changes in the outlet stream composition were significant. The concentration of C<sub>2</sub> hydrocarbons (mainly ethane) was increased in contrast with those of C<sub>3</sub> and C<sub>4</sub> hydrocarbons, which were reduced. These changes were stronger over the higher temperature range (240–290 °C).
4. With the Pd/Al<sub>2</sub>O<sub>3</sub> catalyst, the overall methane conversion was 30–50% and the methane conversion to C<sub>2</sub>–C<sub>4</sub> hydrocarbons reached 22%. Moreover, the solid deposit formation radically slowed down.

## Acknowledgements

This work was financially supported by ERA-NET CHEMISTRY (Decision nr 139/ERA-NET/2008) and by Ministry of Science and Higher Education nr N N205 0829 33

## References

- [1] K. Schmidt-Szałowski, S. Jodzis, K. Krawczyk, M. Młotek, A. Górka, *Curr. Top. Catal.* 5 (2006) 39–68.
- [2] K. Zhang, B. Eliasson, U. Kogelschatz, *Ind. Eng. Chem. Res.* 41 (2002) 1462–1468.
- [3] K. Schmidt-Szałowski, K. Krawczyk, M. Młotek, *Plasma Process. Polym.* 4 (2007) 728–736.
- [4] F.-J. Spiess, S.L. Suib, K. Irie, Y. Hayashi, H. Matsumoto, *Catal. Today* 89 (2004) 35–45.
- [5] C.-J. Liu, B. Eliasson, B. Xue, Y. Li, Y. Wang, *React. Kinet. Catal. Lett.* 74 (2001) 71–77.
- [6] S.-S. Kim, H. Lee, J.-W. Choi, B.-K. Na, H.K. Song, *Catal. Commun.* 8 (2007) 1438–1442.
- [7] S.S. Kim, J. Choi, J. Kim, H. Lee, H.K. Song, *J. Ind. Eng. Chem.* 11 (4) (2005) 533–539.
- [8] S.-S. Kim, B. Kwon, J. Kim, *Catal. Commun.* 8 (2007) 2204–2208.
- [9] K. Schmidt-Szałowski, A. Górka, M. Młotek, *J. Adv. Oxid. Technol.* 9/2 (2006) 215–219.
- [10] A.A. Khassin, B. Pietruszka, M. Heintze, V.N. Parmon, *React. Kinet. Catal. Lett.* 82 (1) (2004) 131–137.
- [11] M. Heintze, B. Pietruszka, *Catal. Today* 89 (2004) 21–25.
- [12] T. Nozaki, W. Fukui, K. Ozaki, *Energy Fuels* 22 (2008) 3600–3604.
- [13] S.A. Nair, T. Nozaki, K. Okazaki, *Chem. Eng. J.* 132 (2007) 85–95.
- [14] Th. Hammer, Th. Kappes, M. Baldauf, *Catal. Today* 89 (2004) 5–14.
- [15] A. Indarto, D.R. Yang, J. Palgunadi, J.-W. Choi, H. Lee, H.K. Song, *Chem. Eng. Process.* 47 (2008) 780–786.
- [16] B. Eliasson, C. Liu, U. Kogelschatz, *Ind. Eng. Chem. Res.* 39 (2000) 1221–1227.
- [17] T. Jiang, Y. Li, C.-J. Liu, G.-H. Xu, B. Eliasson, B. Xue, *Catal. Today* 72 (2002) 229–235.
- [18] H.K. Song, J.-W. Choi, S.H. Yue, H. Lee, B.-K. Na, *Catal. Today* 89 (2004) 27–33.
- [19] C. Liu, R. Mallinson, L. Lobban, *J. Catal.* 179 (1998) 326–334.
- [20] C.L. Gordon, L.L. Lobban, R.G. Mallinson, *Catal. Today* 84 (2003) 51–57.
- [21] X. Zhang, B. Dai, A. Zhu, W. Gong, Ch. Liu, *Catal. Today* 72 (2002) 223–227.
- [22] A.N.A.S. Istadi, *Fuel* 85 (2006) 577–592.
- [23] X.-S. Li, A.-M. Zhu, K.-J. Wang, Y. Xu, Z.-M. Song, *Catal. Today* 98 (2004) 617–624.
- [24] M. Kraus, W. Egli, K. Haffner, B. Eliasson, U. Kogelschatz, A. Wokaun, *Phys. Chem. Chem. Phys.* 4 (2002) 668–675.
- [25] H.K. Song, H. Lee, J.-W. Choi, B.-K. Na, *Plasma Chem. Plasma Process.* 24 (1) (2004) 57–72.
- [26] Y. Yang, *Plasma Chem. Plasma Process.* 23 (2003) 327–346.
- [27] M. Młotek, J. Sentek, K. Krawczyk, K. Schmidt-Szałowski, *Appl. Catal. A* 366 (2009) 232–241.